

Mechanical and Wear Properties of CoNiAlSiSb and CoNiAlSiIn Ferromagnetic Shape Memory Alloys: An Experimental Assessment

Yusuf Kanca 

Hitit University, Faculty of Engineering, Department of Mechanical Engineering, Corum, Turkey

ABSTRACT

CoNiAl-based ferromagnetic shape memory alloys (FSMAs) are used in various engineering fields but still, need to be improved for tribological applications. In the present study, the dry sliding wear behavior of CoNiAlSiSb and CoNiAlSiIn FSMAs was investigated as they were articulated against an alumina abrasive ball using a ball-on-disk tribometer. The experiments were carried out at a load of 20 N, a sliding velocity of 20 mm/s, and a sliding distance of 250 m. The worn surfaces were assessed using a scanning electron microscope (SEM) and energy-dispersive X-ray spectroscopy (EDS). The mechanical properties of the CoNiAl-based FSMAs were investigated using the nanoindentation technique. The results showed that as compared to CoNiAlSiSb, CoNiAlSiIn FSMA showed a 42% increase in Young's modulus and a 10% increase in microhardness. The mean coefficient of friction (COF) of CoNiAlSiIn (0.56) was observed to be slightly lower than that of CoNiAlSiSb (0.58). The higher hardness and elastic modulus of CoNiAlSiIn than CoNiAlSiIn caused only a 7% increase in wear resistance. The operative wear mechanisms were abrasion, adhesion, plastic deformation, and micro crack-induced delamination. In conclusion, even though the difference in the tribological performance of the two FSMA surfaces was fairly small, CoNiAlSiIn exhibited better results and thereby would be preferable in possible tribological applications.

Keywords:

CoNiAl; Shape memory alloy; Antimony; Indium; Wear and friction

INTRODUCTION

Shape memory alloys (SMAs) are a sort of smart material owing to the shape memory effect (SME) that is caused by thermoelastic martensitic transformation. The SME can be induced by stress, temperature, or magnetic field. The SMAs triggered by stress and temperature can only induce a low response frequency. But, ferromagnetic SMAs (FSMAs) can cause the combination of a large magnetic-field induced strain and a possible rapid response time [1, 2]. This makes FSMAs suitable for a wide range of applications, such as actuators and sensors. Similar to conventional SMAs, ferromagnetic SMAs (FSMAs) such as NiMnGa, FePd, FePt, NiFeGa, CoNiGa, and CoNiAl [3-5] undergo martensitic phase transformation with the application of stress or by changing temperature.

CoNiAl alloys seem promising for FSMA applications due to their cheap constituents as compared to commonly used NiTi and Cu-based SMAs, and FSMAs

[6]. It is also possible to obtain enough ductility through thermal treatments [7]. Moreover, martensitic transformation and Curie temperatures can independently be tailored over a large composition. [8]. CoNiAl has found applications in the aerospace, automotive, electronics, and biomedical industries [9, 10]. Although there exist some studies investigating the wear behavior of NiTi SMAs [11, 12], limited research is available about the wear performance of CoNiAl FSMAs. Liu et al. (2022) [13] recently investigated the tribological performance of CoNiAl FSMAs coatings synthesized on 38CrMoAl by laser cladding method. The researchers observed the coefficient of friction (COF) of 0.5, the specific wear rate of $5.9 \times 10^{-5} \text{ mm}^3/\text{Nm}$, and the abrasive, adhesive, and oxidation wear mechanism.

Antimony (Sb) and indium (In) are reported to be kinds of elements with high anti-wear properties [14-16], and thus may be considered in CoNiAl-based FSMAs.

Article History:

Received: 2022/12/20

Accepted: 2023/02/27

Online: 2023/03/31

Correspondence to: Yusuf Kanca,
Department of Mechanical Engineering,
Faculty of Engineering, Hitit University,
19030, Corum, Turkey.
E-mail: yusufkanca@hitit.edu.tr
Phone: +90(364) 219 1235

The main purpose of this study is to investigate the wear and friction performance of two different FMSAs (CoNiAlSiSb and CoNiAlSiIn), which has not been researched yet. This study provides dry-sliding reciprocating wear and friction knowledge of the aforementioned materials using a ball-on-disk test configuration. The wear mechanisms were examined by scanning electron microscope (SEM) and energy dispersive X-ray spectroscopy (EDS) technique. The nanohardness and elastic modulus were also determined using nanoindentation tests.

MATERIALS AND METHODS

CoNiAlSiSb and CoNiAlSiIn FMSAs were prepared using the vacuum induction melting process, as explained elsewhere [17]. In brief, the mixture of Co and Ni elements was initially melted in the crucible under an argon atmosphere, followed by adding and melting other elements in the crucible. The molten metal was then cast into preheated ceramic molds and left to cool at room temperature. The chemical composition of CoNiAl-based FMSAs, analyzed using energy-dispersive spectroscopy (EDS) technique, is provided in Table 1.

Table 1. Chemical composition (wt.%) of CoNiAl-based FMSAs used in the current study.

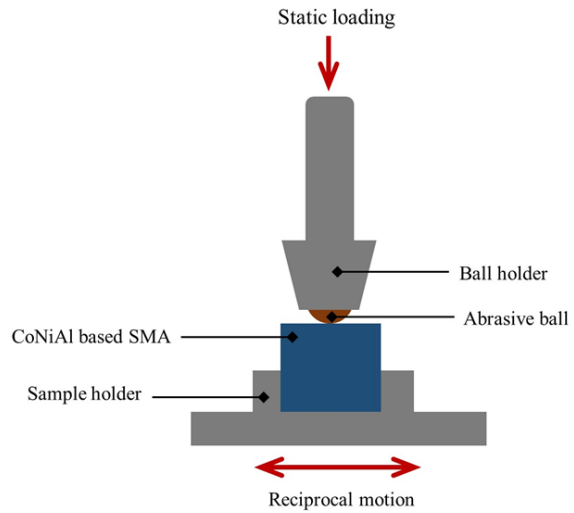
Material	Co	Ni	Al	Si	Sb	In
CoNiAlSiSb	43.30	41.11	7.56	2.40	5.63	-
CoNiAlSiIn	43.39	41.43	8.67	2.44	-	4.07

Cylindrical samples (nominal diameter 11.5 mm, thickness 4 mm) were cold-mounted. Grinding was applied to the surfaces of the samples using 320-, 600-, 800-, 1000-, 1200- and 2500-grit SiC papers, followed by polishing with 1 μ m diamond paste. The nanoindentation tests were carried out using a Hysitron TI-950 TriboIndenter (Germany) equipped with a Berkovich-tip, under a peak load of 5 mN using a trapezoidal function (loading at a constant rate in 5 s, holding for 2 s, and unloading in 5 s). The nanohardness and reduced elastic modulus (E_r) of the samples were determined based on Oliver and Pharr analysis method and E_r is related to Young's Modulus [18, 19]:

$$\frac{1}{E_r} = \frac{(1-\nu_i^2)}{E_i} + \frac{(1-\nu^2)}{E} \quad (1)$$

Where E_i and ν_i are Young's modulus and Poisson's ratio of the indenter, and E and ν are Young's modulus and Poisson's ratio of the test materials. Microhardness was measured by a Vickers pyramid-tip device (Q10, ATM Qness GmbH, Austria) using a 100 g load and 15 s dwell time.

Wear tests were carried out using a customized ball-on-disk type tribometer. The tests were performed against an alumina ball (diameter 6 mm) at room temperature in



Test conditions	
Load	20 N
Sliding speed	20 mm/s
Stroke	5 mm
Sliding distance	250 m
Test temperature	Ambient

Figure 1. A schematic of the tribometer and a summary of the test conditions.

dry sliding conditions. The average relative humidity of the surrounding air was 60-65%. The test parameters were chosen after performing several preliminary experiments, as follows: an applied load of 20 N, a stroke length of 5 mm, a sliding speed of 20 mm/s, and a sliding distance of 250 m. The average surface roughness (R_a) of the samples was $0.170 \pm 0.04 \mu\text{m}$. The friction force was recorded at 40 Hz using a data acquisition system and was then used to calculate the COF (as the ratio of friction force to test load). Mean COF was quantified by averaging the dynamic COFs recorded during the wear test. Experiments were performed in triplicate. A schematic of the tribometer and a list of test parameters are provided in Fig. 1.

The wear track profiles and R_a values were obtained using a 2D profilometry (MarSurf M300, Germany). The wear volume was calculated from the wear track profiles as detailed in previous studies, such as [20]. Then, the wear rate (W) was quantified using the following equation:

$$W = \Delta V / (FS) \quad (2)$$

Where ΔV : Worn volume (mm^3), F : Applied load (N), and S : Sliding distance (m).

Following the experiments, the worn surfaces were characterized using a scanning electron microscope (SEM) (Thermo Scientific Apreo S) equipped with EDS.

RESULTS AND DISCUSSION

Nanoindentation Analysis

The nanohardness, modulus of elasticity, and microhardness values of both FSMAs are given in Table 2. CoNiAlSiIn showed superior nanohardness and reduced elastic modulus as compared to CoNiAlSiSb. The Young's modulus was calculated using Eq. (1) and the Poisson's ratio of the FSMA samples was taken as 0.25 during the conversion. Young's modulus corresponded to a higher value for CoNiAlSiIn (58.15 GPa) than CoNiAlSiSb (40.92 GPa), with an increase of 42%. The finding is aligned with the research by Li et al. (2017) [21]. They reported that Co35Ni35Al30 has a martensite elastic modulus of 36 GPa in [100] orientation and an austenite elastic modulus of 9 GPa in [100] orientation at room temperature. Moreover, the microhardness of CoNiAlSiIn (335.17 HV_{0.1}) was observed to be 10% greater than that of CoNiAlSiSb (303.60 HV_{0.1}). Liu et al. (2022) observed the microhardness of CoNiAl coating at about 440-467 HV_{0.3}. The hardness of CoNiCuAlGaIn alloy measured by Gerstein et al. (2018) [5] yielded a hardness of 450 HV_{0.2}. This difference in hardness is thought to be caused by elemental distribution.

Table 2. Nanoindentation and microhardness results of CoNiAl-based FSMAs.

Material	Nanohardness, H (GPa)	Reduced elastic modulus, E _r (GPa)	Young's modulus, E (GPa)	Microhardness, HV _{0.2}
CoNiAlSiSb	6.03 ± 0.27	42.05 ± 0.95	40.92 ± 0.96	303.60 ± 16.13
CoNiAlSiIn	6.92 ± 0.60	58.83 ± 4.69	58.15 ± 4.90	335.17 ± 12.65

Friction and Wear Behavior

The tribological performance of CoNiAl-based FSMAs was investigated using a ball-on-disk tribometer at 20 N applied load and 250 m sliding distance in dry-sliding conditions. The dynamic coefficient of friction (COF) was recorded during the wear experiments. The obtained COF versus sliding time is demonstrated in Fig. 2, and the mean COF is provided in Table 3.

At the start of testing, the COFs of both test groups were found to be around 0.35. Then, the COFs were rapidly increased to 0.45 for CoNiAlSiIn and 0.49 for CoNiAlSiSb at approximately 15 min of testing. Then, the COF gradually increased to 0.65 over testing. The increased surface roughness may be responsible for the continuous COF increment (Fig. 2), as reported by other researchers [20, 22]. After wear testing, the R_a of CoNiAlSiSb and CoNiAlSiIn increased by 12.9 and 12.4 fold, respectively. The increase in the R_a and thereby COF were greater in CoNiAlSiSb FSMA. COF rise over time may also be attributed to the increased contact area. A slightly greater wear track dimensions were observed in CoNiAlSiSb FSMA (Table 3), which refers to a larger

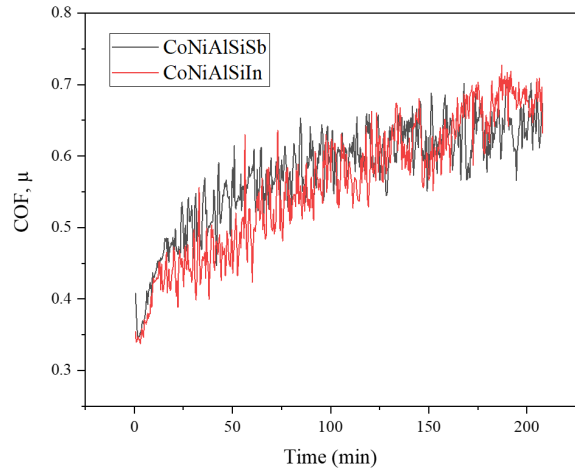


Figure 2. Friction coefficient as a function of time, obtained from the rubbing surfaces between CoNiAl-based FSMAs and the abrasive ball.

articulating surface area. The more the articulating surface area, the greater the COF increment because the relative movement became more difficult at the increased articulating surface area. Therefore, the mean COF of CoNiAlSiIn (0.56±0.02) was observed to be lower than CoNiAlSiSb (0.58±0.03).

Fig. 3 shows the wear profiles of CoNiAl-based SMAs, acquired from a 2D profilometry. The wear track dimensions of CoNiAlSiIn (width 1451 μm, depth 88.86 μm) was slightly smaller than that of CoNiAlSiSb (width 1478 μm, depth 91.63 μm). The drops in the wear track width and depth were 1.8% and 3.0%, respectively. Table 3 shows the wear volume and specific wear rate results, obtained from the wear tracks. The wear volume of CoNiAlSiIn (0.419 mm³) was found to be lower than that of CoNiAlSiSb (0.448 mm³). This is because the higher surface hardness and modulus of elasticity (see Table 2) enabled an improvement in the wear volume. The specific wear rates of the tested FSMAs were calculated using Eq. (2). The wear rate of Co-

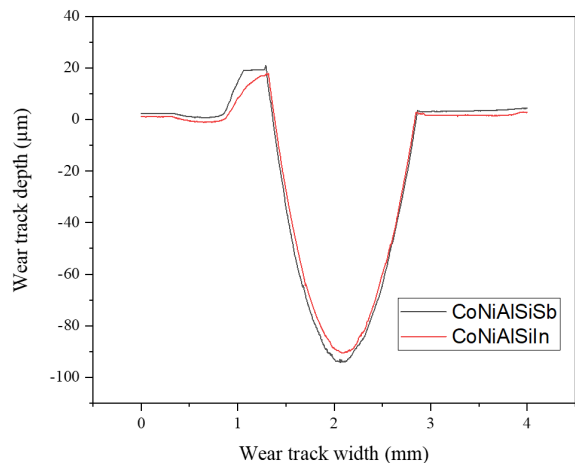


Figure 3. 2D wear track profiles of CoNiAl-based FSMAs, subjected to the wear experiments at 250 m sliding distance.

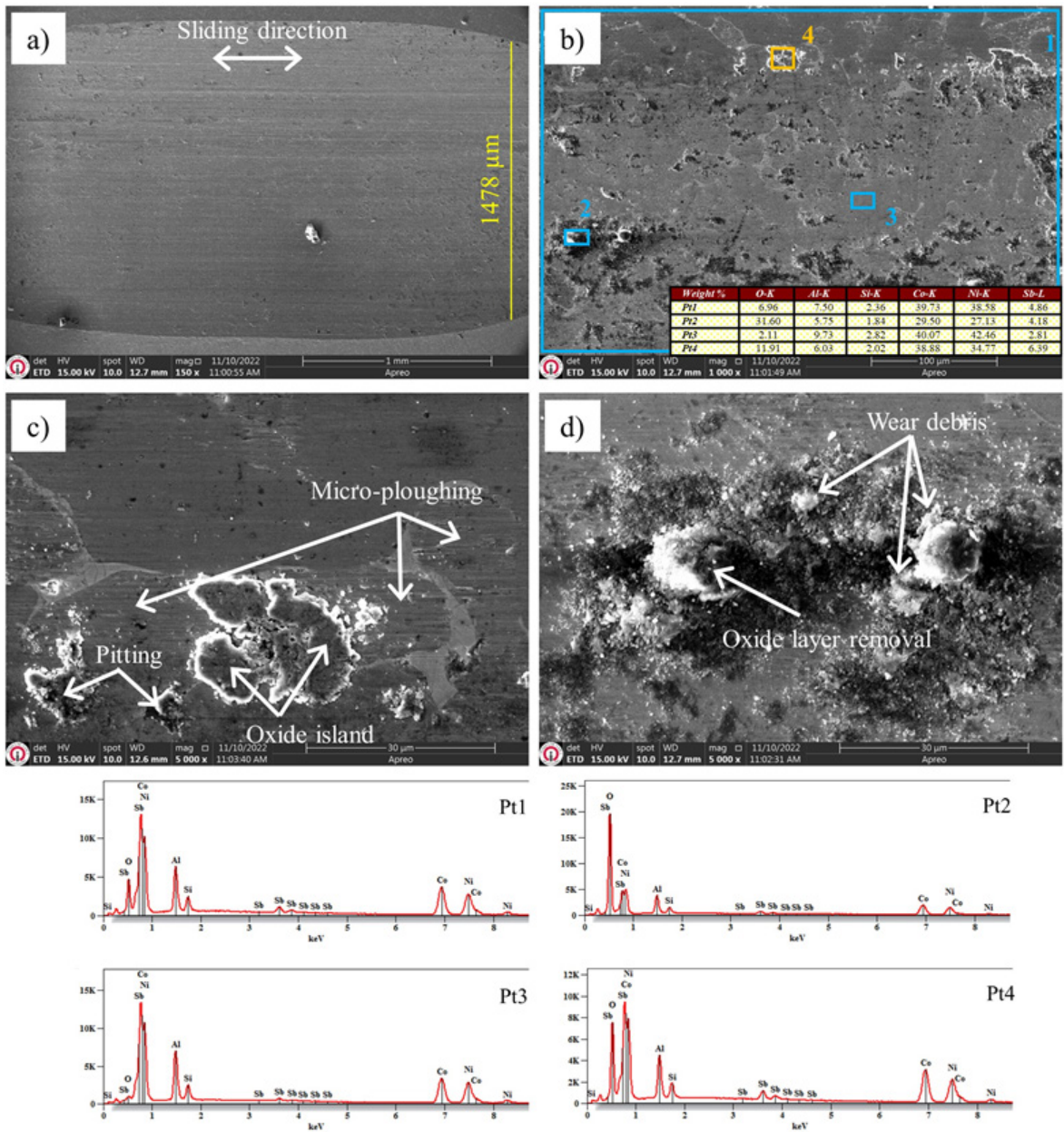


Figure 4. SEM equipped with EDS analyses of CoNiAlSiSb FSMA, subjected to wear testing at the load of 20 N and the sliding distance of 250 m.

NiAlSiIn ($8.38 \times 10^{-5} \text{ mm}^3/\text{Nm}$) was observed to be lower than that of CoNiAlSiSb ($8.96 \times 10^{-5} \text{ mm}^3/\text{Nm}$). The specific wear rates of CoNiAl-based FSMAs are comparable to the specific wear rate of CoNiAl alloy ($5.9 \times 10^{-5} \text{ mm}^3/\text{Nm}$) reported by Liu et al. (2022) [13]. Also, the wear rates observed in the present work are superior to NiTi SMAs observed by Levitant-Zayonts et al. (2019) [23] at a sliding distance of 285 m ($7.0\text{--}17.5 \times 10^{-5} \text{ mm}^3/\text{Nm}$). The authors also showed

a decreasing specific wear rate at an increased sliding distance. Specific wear rates of CoNiAlSiSb and CoNiAlSiIn FSMAs at various normal loads and sliding distances may be investigated in future work. The wear resistance is defined as the rate of 1/ specific wear rate and the wear resistance of CoNiAlSiIn FSMA was 7% higher than CoNiAlSiSb FSMA. Furthermore, there was found to be some surface damage on the alumina ball upon visual inspection.

Table 3. Mean surface roughness, average COF, width, depth, wear volume, and specific wear rate of wear tracks.

Material	Mean surface roughness, R_a (μm)	Average COF, μ_{av}	Width of wear track (μm)	Depth of wear track (μm)	Wear volume, ΔV (mm^3)	Specific wear rate, W ($10^{-5} \text{ mm}^3/\text{Nm}$)
CoNiAlSiSb	2.367 ± 0.285	0.58 ± 0.03	1478 ± 151	91.63 ± 7.73	0.448 ± 0.025	8.96 ± 0.50
CoNiAlSiIn	2.280 ± 0.205	0.56 ± 0.02	1451 ± 68	88.86 ± 8.61	0.419 ± 0.013	8.38 ± 0.26

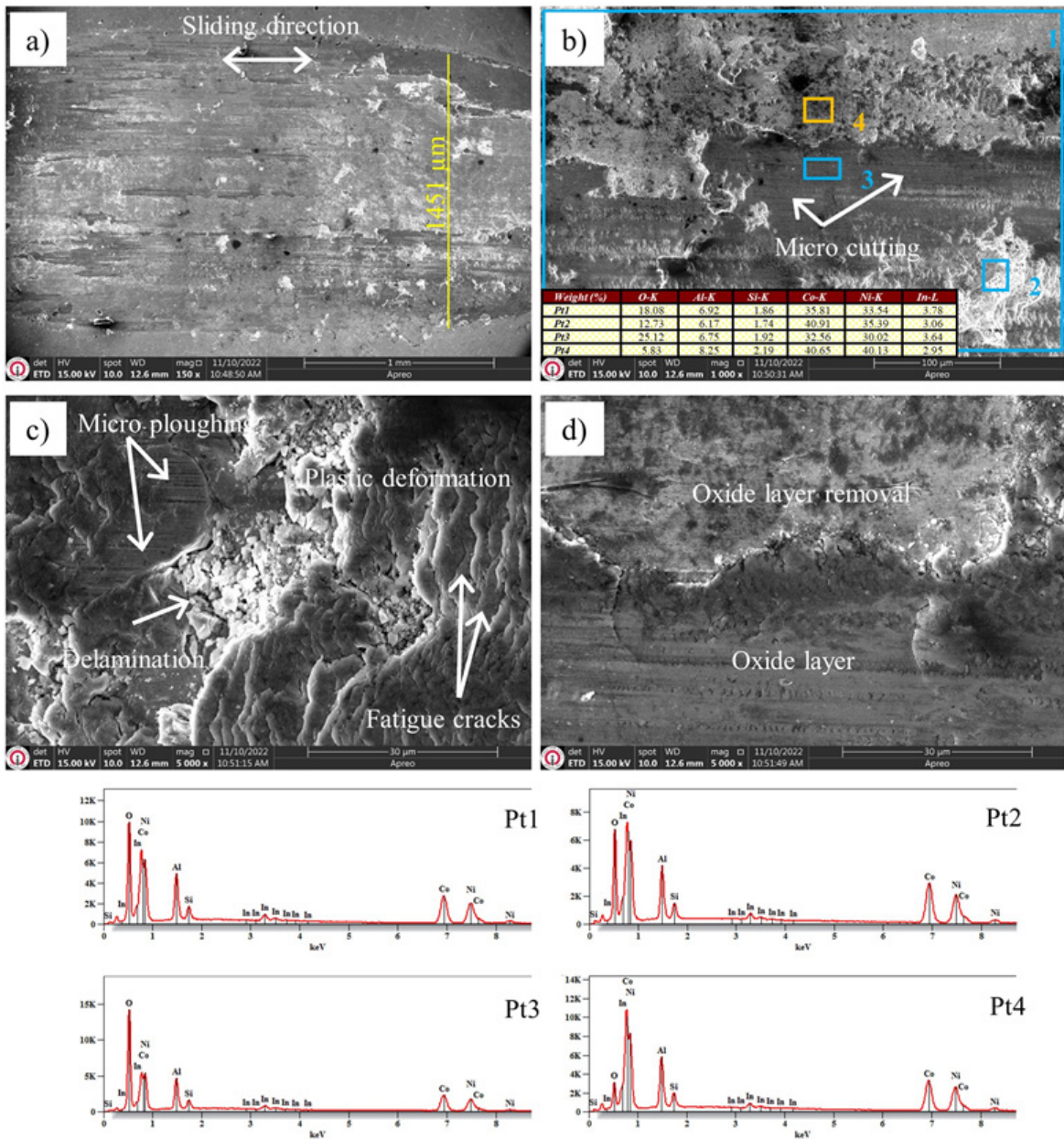


Figure 5. SEM equipped with EDS analyses of CoNiAlSiIn FSMA, subjected to wear testing at the load of 20 N and the sliding distance of 250 m.

Worn Surface Analysis

The worn surfaces of CoNiAl-based FSMA were analyzed using SEM-EDS technique (Figs. 4 and 5). The wear track widths obtained from the SEM images (Figs. 4a and 5a) were observed to be in good agreement with those measured from the 2D wear track profiles (Fig. 3 and Table 3). The worn surfaces of CoNiAlSiSb and CoNiAlSiIn FSMA found evidence of plastic deformation and micro-ploughing. Therefore, the dominant wear mechanisms were adhesion and abrasion. EDS spectra showed the elements of CoNiAl-based FSMA and also oxygen (Figs. 4b and 5b). Oxygen is mainly caused by the formation of oxides due to temperature increase at the bearing contact in dry sliding conditions. The oxide layer

was removed from the surface under repetitive loads (Fig. 5d). Transverse cracks on the wear track of CoNiAlSiIn FSMA occurred due to repetitive loads experienced during the wear test, which indicate the presence of fatigue wear (Fig. 5c). The SEM images also showed microcracking and delamination on the worn surfaces of both CoNiAl-based FSMA (Figs. 4c and 5c).

CONCLUSIONS

In the present study, the wear and friction properties of two different FSMA (CoNiAlSiSb and CoNiAlSiIn) were investigated using a ball-on-disk test apparatus in dry sliding conditions. The following conclusions can be drawn:

1- CoNiAlSiIn FSMA found a 42% increase in Young's modulus and a 10% increase in the microhardness than CoNiAlSiSb FSMA.

2- The mean COF obtained from CoNiAlSiIn FSMA (0.56) was slightly lower than that of CoNiAlSiSb FSMA (0.58).

3- The higher hardness and elastic modulus of CoNiAlSiIn as compared to CoNiAlSiIn resulted in a 7% increase in wear resistance.

4- Abrasion, adhesion, plastic deformation, and micro crack-induced delamination were the operative wear mechanisms in both CoNiAlSiSb and CoNiAlSiIn FSMA.

5- Even though there was found to be a slight difference between the wear and friction performance of the two FSMA, the superior values obtained from CoNiAlSiIn would support its preference in possible tribological applications.

ACKNOWLEDGMENT

The author received no financial support for the research, authorship, and/or publication of this article.

CONFLICT OF INTEREST

The author approves that to the best of his knowledge, there is not any conflict of interest or common interest with an institution/organization or a person that may affect the review process of the paper.

REFERENCES

- Ullakko K. Magnetically controlled shape memory alloys: A new class of actuator materials. *Journal of materials Engineering and Performance* 5 (1996) 405-409.
- Karaca H, Karaman I, Chumlyakov Y, Lagoudas D, Zhang X. Compressive response of a single crystalline CoNiAl shape memory alloy. *Scripta materialia* 51 (2004) 261-266.
- Chumlyakov YI, Kireeva I, Panchenko EY, Timofeeva E, Pobedennaya Z, Chusov S, et al. High-temperature superelasticity in CoNiGa, CoNiAl, NiFeGa, and TiNi monocrystals. *Russian Physics Journal* 51 (2008) 1016-1036.
- Nespoli A, Biffi CA, Villa E, Tuissi A. Effect of heating/cooling rate on martensitic transformation of NiMnGa-Co high temperature ferromagnetic shape memory alloys. *Journal of Alloys and Compounds* 690 (2017) 478-484.
- Gerstein G, Firstov G, Kosorukova T, Koval YN, Maier H. Development of B2 shape memory intermetallics beyond NiAl, CoNiAl and CoNiGa. *Shape Memory and Superelasticity*. 4 (2018) 360-368.
- Alkan S, Sehitoglu H. Plastic flow resistance of NiTiCu shape memory alloy-theory and experiments. *Acta Materialia* 163 (2019) 173-188.
- Kainuma R, Ise M, Jia C-C, Ohtani H, Ishida K. Phase equilibria and microstructural control in the Ni-Co-Al system. *Intermetallics* 4 (1996) S151-S158.
- Oikawa K, Wulff L, Iijima T, Gejima F, Ohmori T, Fujita A, et al. Promising ferromagnetic Ni-Co-Al shape memory alloy system. *Applied Physics Letters* 79 (2001) 3290-3292.
- Chatterjee S, Thakur M, Giri S, Majumdar S, Deb A, De S. Transport, magnetic and structural investigations of Co-Ni-Al shape memory alloy. *Journal of alloys and compounds* 456 (2008) 96-100.
- Bu F, Xue X, Wang J, Kou H, Li C, Zhang P, et al. Effect of strong static magnetic field on the microstructure and transformation temperature of Co-Ni-Al ferromagnetic shape memory alloy. *Journal of Materials Science: Materials in Electronics* 29 (2018) 19491-19498.
- Qian L, Zhou Z, Sun Q, Yan W. Nanofretting behaviors of NiTi shape memory alloy. *Wear* 263 (2007) 501-507.
- Qian L, Zhou Z, Sun Q. The role of phase transition in the fretting behavior of NiTi shape memory alloy. *Wear* 259 (2005) 309-318.
- Liu C, Cui X, Jin G, Su W, Liu E, Liu J. Study of the mechanical property and tribology property of CoNiAl alloy with dual phase eutectic. *Materials Chemistry and Physics* 294 (2023) 127018.
- Zhao Y, Zhang Z, Dang H. A novel solution route for preparing indium nanoparticles. *The Journal of Physical Chemistry B* 107 (2003) 7574-7576.
- Xu J, Yang S, Niu L, Liu X, Zhao J. Study on Tribological Properties of Antimony Nanoparticles as Liquid Paraffin Additive. *Journal of Tribology* 139(5) (2017) 051801.
- Cao Y, Zhang Y, Yang TY. Effect of Addition of Montmorillonite and Indium Composite Powder on Tribological Properties of 45 Steel Friction Pairs. *Key Engineering Materials: Trans Tech Publ* 866 (2020) 152-160.
- Eskil M, Sahan ZA. Effect of Cryogenic Heat Treatment on Phase Formation in Co38Ni37Al17Si6Sb2 Ferromagnetic Shape Memory Alloy. *Journal of Materials Engineering and Performance* 30 (2021) 7283-7294.
- Oliver WC, Pharr GM. Measurement of hardness and elastic modulus by instrumented indentation: Advances in understanding and refinements to methodology. *Journal of Materials Research* 19(1) (2004) 3-20.
- Oliver WC, Pharr GM. An improved technique for determining hardness and elastic modulus using load and displacement sensing indentation experiments. *Journal of Materials Research* 7 (1992) 1564-1583.
- Kanca Y. Microstructural characterization and dry sliding wear behavior of boride layers grown on Invar-36 superalloy. *Surface and Coatings Technology* 449 (2022) 128973.
- Li P, Karaca HE, Chumlyakov YI. Orientation dependent compression behavior of Co35Ni35Al30 single crystals. *Journal of Alloys and Compounds* 718 (2017) 326-334.
- Carrera-Espinoza R, Figueroa-López U, Martínez-Trinidad J, Campos-Silva I, Hernández-Sánchez E, Motallebzadeh A. Tribological behavior of borided AISI 1018 steel under linear reciprocating sliding conditions. *Wear* 362 (2016) 1-7.
- Levintant-Zayonts N, Starzynski G, Kopec M, Kucharski S. Characterization of NiTi SMA in its unusual behaviour in wear tests. *Tribology International* 137 (2019) 313-323.